Astron. Astrophys. 334, 264–268 (1998)

ASTRONOMY AND ASTROPHYSICS

Imaging studies of localized, ionized flows in the Rosette nebula

C.A. Clayton[1], **J. Meaburn**[2], **J.A. López**[3], **P.E. Christopoulou**[2,4], **and C.D. Goudis**[2,4]

[1] Rutherford Appleton Laboratory, Chilton, Didcot, Oxon OX11 0QX, UK
[2] Department of Physics and Astronomy, University of Manchester, Oxford Road, Manchester M13 9PL, UK
[3] Instituo de Astronomía, UNAM, Apartado Postal, 877, Ensenada, México
[4] Astronomical Laboratory, Department of Physics, University of Patras, GR-26110 Patras, Greece

Received 24 September 1997 / Accepted 6 January 1998

Abstract. Optical ([S II] 6717 & 6731Å, [S III] 9069Å, [O III] 5007Å and Hα + [N II] 6584Å), K–band, H_2 1-0 S(1) 2.122μm and [Fe II] 1.64μm imagery has been obtained of a group of high–speed knots close to the core of the Rosette nebula. A high–speed, high–excitation, bow–shaped structure has been directly imaged in [O III] 5007Å for the first time and is interpreted as a bow shock either at the head of a collimated flow or around a fast–moving molecular bullet. Two candidates for the driving source of these motions have also been identified in a system where no sources were previously known.

Key words: ISM: individual objects: Rosette nebula – ISM: jets and outflows – H II regions – infrared: ISM: lines and bands

1. Introduction

A group of lowly-ionized, high-speed knots have been located in the core of the galactic HII region, the Rosette nebula (Meaburn & Walsh 1986 - hereafter Paper 1).

Clayton & Meaburn (1995) (hereafter Paper 2) have reported the results of volumetric imagery (i.e images in separate ranges of radial velocity) in the light of the line [O III] 5007Å of two of these knots (B & C in Paper 1). One striking result of this previous work was the detection of a high-speed bow-shaped filament surrounding the knot (C) which is approaching the observer with the highest velocity. This filament has an approaching radial velocity of 66 km s^{-1} (Paper 2) with respect to the systemic heliocentric radial velocity. Furthermore, the filament is exceptionally bright in the [O III] 5007Å line but not visible in deep images taken in the light of Hα + [N II] 6548 & 6584 Å . In all respects it is then most unlike the bright rims of similar appearance, that appear on images of this region, which are generated by ionization fronts on the surfaces of irradiated, neutral clouds.

A 'tube' of material appears to connect the two knots. It is referred to as a tube since visually if appears to comprise of a bright ionized skin surrounding a sharply defined column of low (similar to background) emission. The ionized tube also exhibits an approaching radial velocity (Paper 2).

Various mechanisms for the creation of the high-speed phenomena observed were considered in Paper 2 but were inconclusive primarily because the source driving these motions had not been identified.

The purpose of the work described in the present paper is firstly to identify the driving source of the flows, and consequently the mechanism for their creation, and secondly to further investigate the nature of the unusual, bow–shaped [O III] 5007Å filament. The optical data is uncalibrated and hence this paper is essentially descriptive.

Throughout this paper, a distance to the Rosette nebula of 1800 pc is assumed (Davies et al. 1978).

2. Observations and results

2.1. CCD imagery

CCD images of the two knots and the surrounding region (4′ × 4′) were obtained in the light of [S II] 6717 & 6731Å, [S III] 9069Å, [O III] 5007Å, and Hα+ [N II] 6548 & 6584 Å using a 1024x1024 Thompson CCD (with a pixel size of 20μm, equating to 0.26″ on the sky) on the 2.2-m UNAM telescope at the San Pedro Mártir Observatory, Mexico, with the MANMEX filter camera (López et al. 1995). The effective exposures of the images shown in Fig. 1 were 1200s, 3000s, 1200s & 600s for the [S II] 6717 & 6731Å, [S III] 9069Å, [O III] 5007Å and Hα + [N II] 6548 & 6584 Å
images respectively (after alignment and co–addition of two separate CCD images in the case of the [S III] 9069Å & [O III] 5007Å observations). Observations of a standard star with which to calibrate these images were not available. The seeing varied between 1″ – 2″ during these observations.

The appearance of knot B varies little with wavelength. However, this is not the case with knot C. It is shown in Fig. 1 that this knot is comprised of three distinct components. The most easterly of these ($V_{\rm HEL} = -31$ km s^{-1} - Paper 2) is bright in the Hα + [N II] 6548 & 6584 Å and [S II] 6717 & 6731Å images but is almost undetected in the [O III] 5007Å observations. Similarly, the most westerly component
($V_{\rm HEL} = +1$ km s^{-1}- Paper 2) is bright in [O III] 5007Å and Hα + [N II] 6584Å but faint in [S II] 6717 & 6731Å.

The 'tube' feature near knot B (see Fig. 2), bright in [O III] 5007Å and Hα + [N II] 6548 & 6584 Å is not detected in [S II] 6717 & 6731Å.

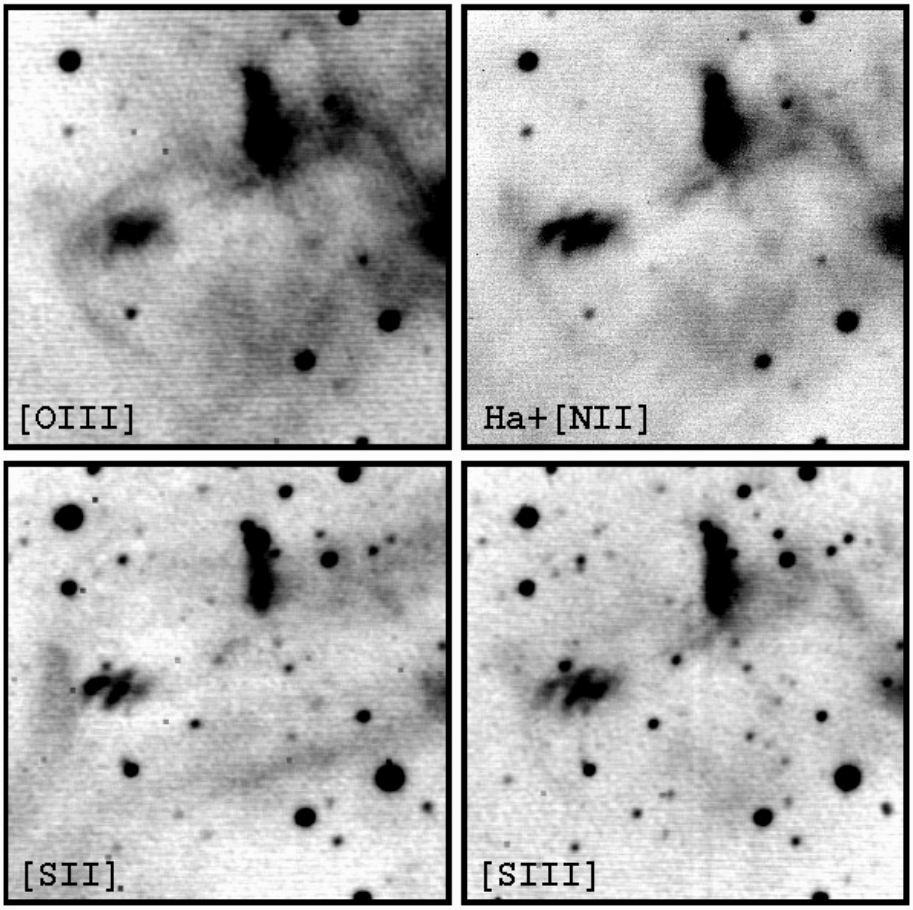

Fig. 1. CCD images of the localized, ionized flow system in the light of [O III] 5007Å, Hα + [N II] 6548 & 6584 Å , [S II] 6717 & 6731Å and [S III] 9069Å. North is to the top. Knot B is just above the centre of each image. Knot C is to the left of centre of each image. The field is $4'$ by $4'$.

The high-speed, bow-shaped filament, which has been directly imaged for the first time (see Fig. 1) with these observations, emits strongly at [O III] 5007Å but is not detected at the other wavelengths.

2.2. K-band imagery

K-band images of the region immediately to the west of knot B were obtained using the IRCAM3 infrared camera on UKIRT. In the observing mode used, the detector had 256 $\times$ 256 pixels, each $0.3''$ across. Knot C was not within the field of view. The exposure of each image was 80 seconds. The standard star FS 13 was used for photometric calibration.

The K-band image shown in Fig. 3 reveals two bright sources, S_1 & S_2 (K mags. 16.9 & 16.5 respectively) offset from knot C by 134 & 144 arcsec (1.2 & 1.3 pc) respectively and directly along the line of the ionized tube. These two candidates for the driving source of the observed motions are indicated in Fig. 2.

These sources are also visible in the CCD images presented in Fig. 1. S_2 was barely detected at [S II] 6717 & 6731Å compared with S_1, but is strong at wavelengths longer than 9000Å. Hence, S_2 is the redder of the two candidate sources.

The K magnitudes of these objects are not dissimilar to those of the energy sources of HH objects measured by Moneti & Reipurth (1995), once the observed magnitudes are adjusted to compensate for the difference in distance to each object. For example, ignoring the effects of extinction, the driving source of HH34 would have a K magnitude of 14.5 at the distance of the Rosette nebula.

2.3. H_2 1-0 S(1) 2.122μm and [FeII] 1.644μm imagery

H_2 1-0 S(1) 2.122μm and [FeII] 1.644μm images were obtained of knots B and C using the IRCAM3 infrared camera on UKIRT. Each is a mosaic made up of 18 30-second on-source exposures (giving a total exposure time of 540 seconds) with IRCAM3 working in the same mode as for the K-band observations. An associated 2.1μm continuum image was also obtained for the purposes of continuum subtraction.

The two candidate driving sources of the motions observed in the K-band image discussed above (S_1 & S_2) were not within the field of view of these observations.

After continuum subtraction, neither image shows any emission from either of the knots. This is somewhat surprising since knot C is bright in [S II] 6717 & 6731Å. [Fe II] 1.64μm emission comes from low-excitation gas, similar to that traced by optical [S II] 6717 & 6731Å but suffering much less from differential extinction. The absence of H_2 and [Fe II] 1.64μm emission is discussed further in Sect. 3.2.

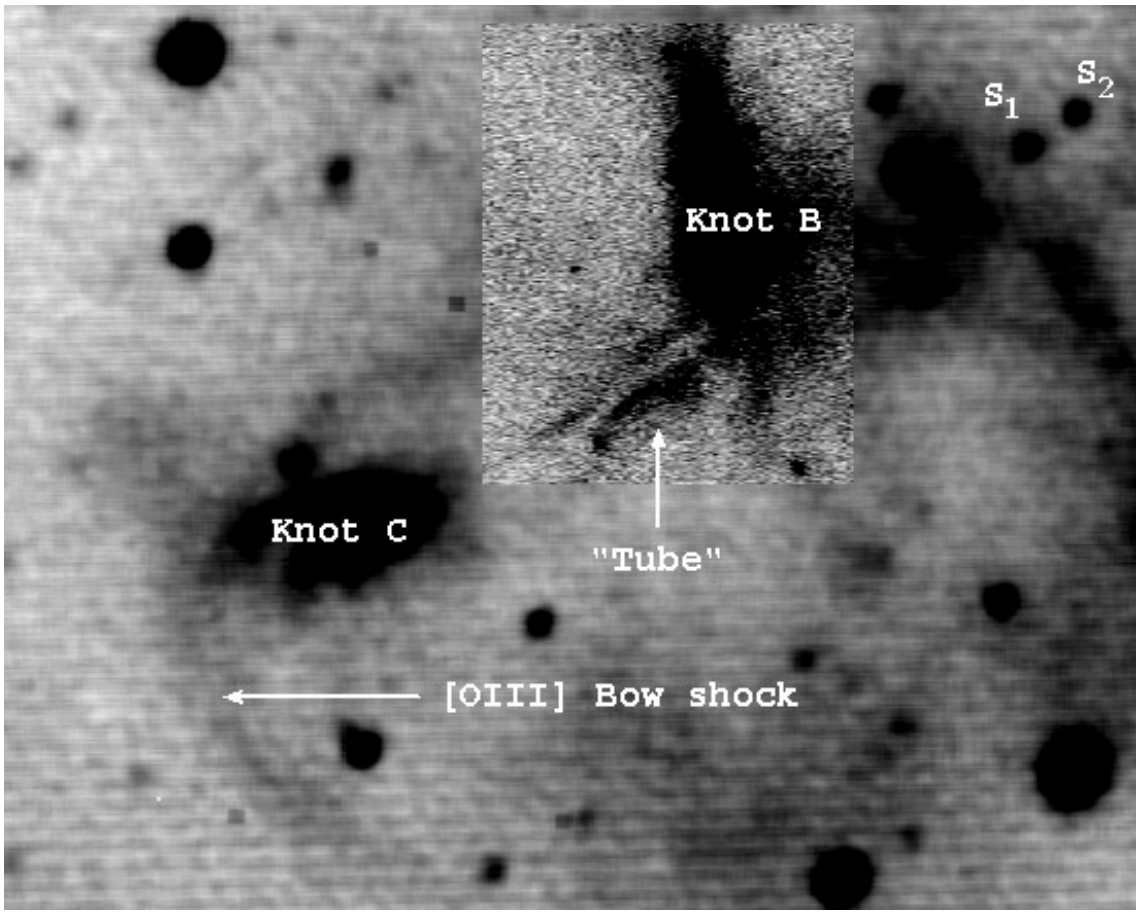

Fig. 2. A composite image of the system showing all important components simultaneously. The main image is the co-addition of the [O III] 5007Å & [S II] 6717 & 6731Å images in Fig. 1, allowing the [O III] 5007Å bow shock, the working surface of the flow (knot C) and the candidate driving sources S_1 and S_2 to be seen simultaneously. An Hα + [N II] 6548 & 6584 Å image of knot B and the ionized tube, obtained during good seeing on the WHT (see Paper 2), has been scaled and aligned and is superimposed on top of the main image. North is to the top.

3. Discussion

3.1. CCD imagery

Direct imagery of the bright filament is presented for the first time in the [O III] 5007Å image in Fig. 1. The authors believe this filament to be a bow shock on account of both its morphology but more importantly its kinematic structure (Paper 2). The shape of part of this feature was previously determined in Paper 2 by constructing an indirect image from spectral observations.

The orientation of the bow shock clearly indicates the motion of a bullet or finger of material eastwards and also rules out an interpretation of the motions observed in Paper 2 involving high speed flows driven around globules by the un-shocked wind from the central 04V and O6V stars which radiatively ionizes the Rosette nebula.

HH objects traditionally have weak high excitation lines such as [O III] 5007Å. However, other examples of high excitation HH objects do exist (e.g. Ogura & Noumaru 1994, Noriega-Crespo, Garnavich & Raga 1993) and these are usually interpreted, as here, in terms of excitation by strong shocks. The study of plane parallel shock models has shown that the excitation of [O III] 5007Å requires shock velocities of $\geq$ 80 – 100 km s^{-1} (Hartigan, Raymond & Hartmann 1987). However, the Hα/[NII] ratio of 1.8 in knot C (see Paper 1) does indeed indicate a shock velocity of about 100 km s^{-1} (see Paper 2).

The strong [S II] 6717 & 6731Å emission in the eastern component of knot C is consistent with collisional ionization by shocks. Low resolution spectroscopy of knot C (Paper 1) and the resultant [S II]6716/6731Å ratio *vs.* log Hα/[N II] 6548 & 6584 Å diagnostic diagram (after Sabbadin, Minello & Bianchini 1979) also strongly suggest that knot C is collisionally, rather than radiatively ionized.

The low brightness of the knot B 'tube' in the light of [S II] 6717 & 6731Å compared with knot C requires explanation.

In Herbig-Haro objects where one is looking at the low-excitation stellar jet, emission lines are narrow and indicate high radial velocities. In comparison, bow shocks show a the wide range of excitation conditions and large line widths (Hartigan 1994). The low excitation and line widths in stellar jets are usually interpreted as indicating weak shocks orientated at oblique angles to the flow.

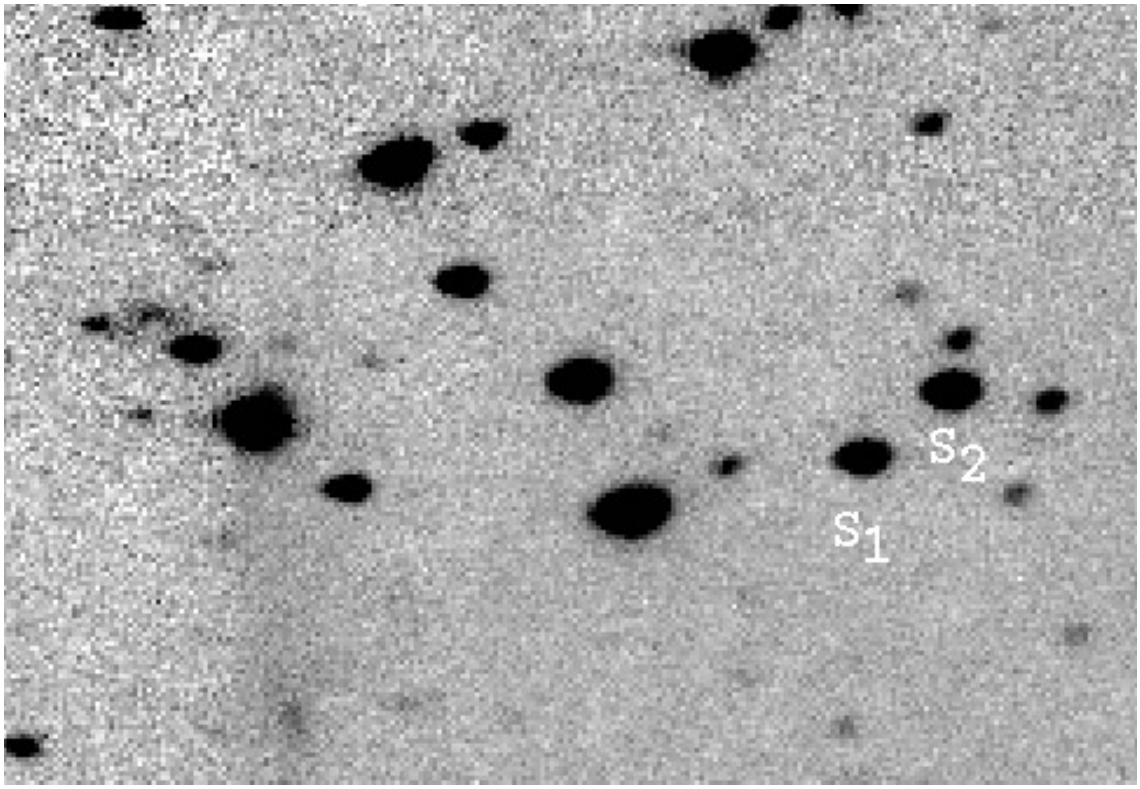

Fig. 3. A subset of a K-band image taken with IRCAM3. The diffuse object to the lower left is Knot B. The two candidate driving sources revealed for the first time in this image are marked (S_1 & S_2). Most of the other bright stars are also visible in the optical and are presumed to be foreground rather than embedded objects. The field size is $74'' \times 51''$.

The velocity images in Paper 2 do show the 'tube' to have only a modest line width and high, negative radial velocity. However, [S II] 6717 & 6731Å lines are bright in stellar jets (Hartigan, Morse & Raymond 1994) and yet very weak in the knot B 'tube' phenomenon. The lack of collisional excitation in the tube may indicate that a "bullet" model for the motions, rather than a moving molecular finger, is more appropriate in this system. This in turn implies an eruptive energy source. Many cases of high-speed bullets forming working surfaces are known (e.g. Cernicharo & Reipurth 1996).

3.2. H_2 1-0 S(1) 2.122μm and [FeII] 1.644μm imagery

H_2 is a useful tracer of shocks with velocities up to 30–50 km s^{-1} (Smith 1993). H_2 emission occurs in the wings of a bow shock where shocks are oblique and thus the shock velocities are low. It can delineate the oblique shocks in bow shock wings and along the interfaces between collimated stellar jets and their molecular surroundings. For shock velocities greater than 30–50 km s^{-1}, H_2 is dissociated (Draine, Roberge & Dalgarno 1983).

[FeII] is a tracer of shocks with velocities above about 50 (and up to a few hundred) $\mathrm{km\,s^{-1}}$ (Hollenbach & McKee 1989). [Fe II] 1.64μm emission comes from low-excitation gas, similar to that traced by optical [S II] 6717 & 6731Å lines (both lines being derived from excited levels at similar energies and S I and Fe I atoms have similar ionization potentials). However, [Fe II] 1.64μm suffers from much less differential extinction. [Fe II] 1.64μm emission will occur as jets from young stars strike dense ambient material in planar (rather than bow) shocks. Thus [Fe II] 1.64μm emission will be observed at the head of a bow shock.

The integration time used for the H_2 and [Fe II] 1.64μm imaging is sufficient to detect such emission in many other H-H objects (Davis, Eislöffel & Ray 1994, Davis, Mundt & Eislöffel 1994). The complete lack of H_2 emission might indicate a lack of molecular material i.e. that the motions are caused by a bullet ejected from the driving source at a particular epoch rather than by a moving finger of molecular material motivated by a continuous input of energy. Strong evidence for this kind of behaviour has been seen by Cernicharo & Reipurth (1996). It is also possible that the ambient material is too tenuous to provide observable shocks interactions; no emission in [S II] 6717 & 6731Å is visible from the tube, but the ionized tube is clearly visible in the Hα + [N II] 6548 & 6584 Å images indicating that there has been an interaction with the ambient material. A further explanation might be that the shocks are so strong that H_2 has dissociated. However, if this were the case, one would expect to detect the [Fe II] 1.64μm emission instead. A further possibility in such a large HH–like object is that the post–shock densities are too low for the creation of H_2 molecules (Wolfire & Königl 1991).

Table 1. System parameters

Parameter	Value
Inclination to plane of sky (°)	13 [b]
Star-to-working surface distance (pc)	1.2 - 1.3
Dynamical time scale (yr)	3.4×10^3
Bullet/Jet velocity (km s^{-1})	290 [b]
Kinetic energy in flow (erg)	2.3×10^{44} [a]

[a] Paper 1
[b] Paper2

Theoretical models describing how HH jets might drive molecular outflows fall into two broad categories. The first involves the working surface of a jet sweeping up and accelerating ambient material (e.g. Raga & Cabrit 1993). In the second, material can suffer "lateral entrainment" along the jet/environment boundary. This entrainment usually results in oblique shocks along the interface between collimated stellar jets and their molecular surroundings, which result in H_2 excitation. The lack of H_2 emission may indicate a preference for the first model but again, [Fe II] 1.64μm emission would be expected near knot C.

Finally, the non-detection of molecular hydrogen and [Fe II] 1.64μm emission might simply indicate that there is no bow shock. However, the bow–shaped filament is moving with a high–velocity and shock excitation of some sort would be expected.

3.3. General

High resolution ^{13}CO emission studies show that the Rosette nebula cloud is composed of dense molecular clumps embedded in pervasive molecular gas (Blitz & Stark 1986; Blitz 1987). The most massive structures appear to be gravitationally bound and may have collapsing cores.

Gas photo–ionized by the central OB association is expanding and driving an ionization front into the molecular cloud. Star formation is taking place in this compressed medium (Cox, Deharveng & Leene 1990; Phelps & Lada 1997). Outflow from young stellar objects is common (Schwartz 1983). In the case of Herbig–Haro objects, the existence of shocks indicate that this flow is highly collimated.

If either S_1 or S_2 is the local source that drives the observed motions associated with knot C, then this offers direct evidence that star formation is occurring (the T-Tauri type stars that usually drive these motions have lifetimes of 10^5 yr).

Using the flow velocity and angle to the plane of the sky calculated in Paper 2 together with the observed separation of knot C (the working surface) and the proposed driving source, a dynamical time scale of 3.4×10^3 yr is inferred. Parameters for this system of knots are given in Table 1.

Cernicharo & Reipurth (1996) have observed CO bullets moving with space velocities of 240 $\mathrm{km\,s^{-1}}$ in HH 111. Dynamical timescales of the order of 10^3 yr are typical for HH objects.

4. Conclusions

These further observations of these curious knots provide strong evidence that they comprise part of an HH-like object. The existence of a high-excitation [O III] 5007Å bow shock structure has been substantiated and revealed for the first time through direct imagery and two candidates for the local driving sources of the motions identified. These potential sources are generally aligned with the other major features of the system (the ionized tube, the working surface and the bow shock – see Fig. 2) and offset by $\sim$1 pc. The system would appear to be considerably larger than most HH-objects, similar to M16 HH1 (Meaburn & White 1982), but many of the other system parameters (dynamic time scale, bullet/jet velocity) are consistent with outflow from a young stellar object.

Identification of the stellar types of the two candidate sources will determine which is the driving source.

Star formation has already been detected in the depths of the Rosette molecular cloud further to the east but these observations also provide evidence for star formation close to the region of optical emission i.e. near to surface of the molecular cloud. ISO observations of this region are planned which would enable a determination of the underlying star formation.

Acknowledgements. Some of the data reported here were obtained as part of the UKIRT Service Programme. The authors acknowledge the data analysis facilities provided by the Starlink Project which is run by CCLRC on behalf of PPARC. Also we wish to thank the staff of the San Pedro Mártir Observatory for their excellent assistance during these observations. JAL gratefully acknowledges continuous support from CONACYT and DGAPA-UNAM.

References

Blitz L. & Stark A.A., 1986, ApJ, 300, 89.
Cernicharo J. & Reipurth B., 1996, ApJ, 460, L57.
Clayton C.A. & Meaburn J., 1995, A&A, 302, 202.
Cox P., Deharveng L., Leene A., 1990, A&A, 230, 181.
Davis C.J., Mundt R. & Eislöffel J., 1994, ApJ, 437, L55.
Davis C.J., Eislöffel J. & Ray T.P., 1994, ApJ, 426, L93.
Davis R.D., Elliott K.H., Goudis C.D., Meaburn J. & Tebbutt N.J., 1978, A&AS, 31, 271.
Draine B.T., Roberge W.G. & Dalgarno A., 1993, ApJ, 264, 485.
Hartigan P., 1994, *Low-Excitation HH objects*, PASP Conference Series 57, p94.
Hartigan P., Morse J. & Raymond J., 1994, ApJ, 436, 125.
Hartigan P., Raymond J. & Hartmann L., 1987, ApJ, 316, 323.
Hollenbach D. & McKee C.F., 1989, ApJ, 342, 306.
López J.A., Meaburn J., Carling R. & Murillo J.M., 1995, Technical Reports Series, IAUNAM, MU-95-02.
Meaburn J. & Walsh J.R., 1986, MNRAS, 220, 745.
Meaburn J. & White N.J., 1982, MNRAS, 199, 121.
Moneti A. & Beipurth B., 1995, A&A, 301, 721.
Noriega-Crespo A., Garnavich P.M. & Raga A.C., 1993, AJ, 106, 1133.
Ogura K. & Noumaru J., 1994, AJ, 108, 1427.
Phelps R.L. & Lada E.A., 1997, ApJ, 477, 176.
Raga A.C. & Cabrit S., 1993, A&A, 278, 267.
Sabbadin F., Minello S. & Bianchini A., 1979, A&A, 60, 147.
Schwartz R.D., 1983, ARA&A, 21, 209.
Smith M.D., 1993, ApJ, 406, 520.
Wolfire M.G. & Königl A., 1991, ApJ, 383, 205.